

**POLARIZED STRUCTURE FUNCTIONS:  
THEORY AND PHENOMENOLOGY**

Stefano Forte\*

*Theory Division, CERN,  
CH-1211 Genève 23, Switzerland.*

**Abstract**

We review the theory of polarized structure functions measured in deep-inelastic lepton-nucleon scattering, focusing on the most recent developments. We concentrate on the structure function  $g_1$ , emphasizing the phenomenological problems related to the extraction of the proton and neutron  $g_1(x, Q^2)$  from the data, and to the determination of its moments, especially the first moment. In particular, we discuss the theoretical and experimental uncertainties due to the  $Q^2$  dependence of the data, small and large  $x$  extrapolations, QCD loop corrections, higher twist corrections, and, in connection to neutron experiments, nuclear effects. We also discuss the current status of the sum rules satisfied by the first moment of  $g_1$  and their theoretical interpretation.

Invited talk at the  
*Tennessee International Symposium on Radiative Corrections*  
Gatlinburg, Tennessee, June 1994  
*to be published in the proceedings*

CERN-TH.7453/94  
September 1994

---

\* On leave from INFN, Sezione di Torino, Turin, Italy.

# POLARIZED STRUCTURE FUNCTIONS: THEORY AND PHENOMENOLOGY

Stefano Forte\*

*Theory Division, CERN  
CH-1211 Genève 23, Switzerland*

## ABSTRACT

We review the theory of polarized structure functions measured in deep-inelastic lepton-nucleon scattering, focusing on the most recent developments. We concentrate on the structure function  $g_1$ , emphasizing the phenomenological problems related to the extraction of the proton and neutron  $g_1(x, Q^2)$  from the data, and to the determination of its moments, especially the first moment. In particular, we discuss the theoretical and experimental uncertainties due to the  $Q^2$  dependence of the data, small and large  $x$  extrapolations, QCD loop corrections, higher twist corrections, and, in connection to neutron experiments, nuclear effects. We also discuss the current status of the sum rules satisfied by the first moment of  $g_1$  and their theoretical interpretation.

## 1. Introduction

Polarized deep-inelastic scattering provides a handle on the matrix elements of spin-dependent operators. Because of the intricacies of spin physics, this poses exacting challenges to experimentalists and theorists alike. On the theoretical side, it turns out to be equally hard to extract meaningful physical information from the data, and to understand the significance of that information.

This is perhaps best appreciated by recalling the present status of the measurement of the first moment of the polarized structure function  $g_1$ :

$$\Gamma_1 = \int_0^1 dx g_1(x). \quad (1.1)$$

Among polarized observables, this is the simplest to understand theoretically because there exists only one operator with the appropriate spin at leading twist in the operator-product expansion, the flavor singlet fermionic axial current

$$j_5^\mu = \sum_{i=1}^{N_f} \bar{\psi}_i \gamma_\mu \gamma_5 \psi_i. \quad (1.2)$$

A measurement of  $\Gamma_1$  thus determines (in a way to be discussed extensively below) the (forward) matrix element of  $j_5^\mu$  in the target:

$$\langle p, s | j_5^\mu | p, s \rangle = M s^\mu \Delta \Sigma, \quad (1.3)$$

---

\* On leave from INFN, Sezione di Torino, Italy

where  $p^\mu$ ,  $M$ , and  $s^\mu$  are, respectively, the target four-momentum, mass, and spin (normalized as  $s^\mu s_\mu = -1$ ).

The experimental value of  $\Delta\Sigma$  for a proton target, as given by the various experimental collaborations which have measured it, is displayed in Fig. 1a. All the determinations are compatible within errors; however, the spread of the results indicates how hard these measurements are, and how carefully they should be taken. Actually, the experimental result which has been around longest<sup>2</sup> has been reanalysed by various theoretical groups: the results, shown in Fig. 1b, again display a remarkable degree of variation (also in the error estimate). Finally, it is clear (albeit with hindsight) that whatever the measured value of  $\Delta\Sigma$ , its interpretation will not be obvious: the current  $j_5^\mu$  is not conserved because of the axial anomaly, hence its matrix elements do not directly measure a well-defined conserved quantum number of a physical state.

The increase in experimental precision calls now for a careful reanalysis of the arguments which go into the extraction of structure functions from the data: indeed, the theoretical uncertainty starts to be comparable to the experimental error. On the other hand, after the considerable amount of theoretical work which followed the 1988 EMC experiment,<sup>2</sup> the subtleties involved in the interpretation of the results displayed in Fig. 1 are now largely understood.

In this paper we will concentrate on the phenomenological aspects of structure function measurements, with particular regard to recent developments, and we will briefly summarize the present understanding of their theoretical import. In Sect. 2 we will provide some background on the polarized structure functions  $g_1(x, Q^2)$  and  $g_2(x, Q^2)$ . In Sect. 3 we will then proceed to a discussion of the phenomenology of the proton structure function  $g_1^p$ : first we will discuss the way  $g_1$  is extracted from the data, and review the problems involved in  $Q^2$  dependence and extrapolation in  $x$ ; then we will examine the way  $\Delta\Sigma$  [Eq. (1.3)] is evaluated once  $g_1$  is known, discussing the dependence on weak decay constants and the role of QCD loop corrections. In Sect. 4 we will review the current status of the theoretical interpretation of the data on  $\Delta\Sigma$ , and we will discuss parametrization of polarized parton distributions. In Sect. 5 we will review problems which are of special relevance for the measurement of the neutron structure function  $g_1^n$ , in particular nuclear effects and higher twist effects, and in Sect. 6 we will discuss the significance of the proton and neutron measurements taken together.\*

## 2. The structure functions and their moments

Polarized structure functions are the form factors which parametrize the cross section spin asymmetry for deep-inelastic scattering of polarized leptons off a po-

---

\* For a more detailed introduction to the theory of  $g_1$  in QCD and to theoretical controversies spurred by its measurement the reader is referred to earlier reviews,<sup>7,10</sup> while a recent assessment of the theoretical status of the  $g_1$  measurement is in Ref. 11; for a detailed review of the theory of  $g_2$  see Ref. 12, and for a discussion of other polarized structure functions (relevant for different processes, such as Drell-Yan scattering) Ref. 13.

larized hadronic target  $\frac{d^2(\sigma^{\uparrow\uparrow}-\sigma^{\uparrow\downarrow})}{dQ^2 d\nu}$ ; they are given by the antisymmetric part of the hadronic tensor<sup>15,14</sup>

$$\begin{aligned} iW_A^{\mu\nu} &\equiv \frac{1}{4\pi} \int d^4x e^{iq\cdot x} \langle p, s | J^{[\mu}(x) J^{\nu]}(0) | p, s \rangle \\ &= iM \epsilon^{\nu\nu\rho\sigma} q_\rho \left[ \frac{s_\sigma}{p\cdot q} g_1(x, Q^2) + \frac{s_\sigma p\cdot q - p_\sigma q\cdot s}{(p\cdot q)^2} g_2(x, Q^2) \right] \end{aligned} \quad (2.1)$$

(with standard parton model kinematics), where  $M$  is the target mass. Polarized neutrino scattering is only of academic interest at present, hence we will neglect weak interaction effects, and assume  $J^\mu$  in Eq. (2.1) to be electric currents.

The light-cone expansion of the current product in Eq. (2.1) implies that the moments of the structure functions  $g_1$  and  $g_2$  in the Bjorken limit are given in the nonsinglet case by<sup>15,14</sup>

$$\int_0^1 dx x^{n-1} g_1(x, Q^2) = \frac{1}{2} C_1^n(Q^2) a^n(Q^2) \quad (2.2)$$

$$\int_0^1 dx x^{n-1} g_2(x, Q^2) = \frac{n-1}{2n} [C_2^n(Q^2) d^n(Q^2) - C_1^n(Q^2) a^n(Q^2)]. \quad (2.3)$$

$C_n(Q^2)$  are perturbatively calculable coefficient functions, and  $a_n$  and  $d_n$  are given by matrix elements of the leading twist polarized operators:

$$M a_n s^{\{\sigma p^{\mu_1} \dots p^{\mu_{n-1}}\}} = -\langle p, s | i^{n-1} \bar{\psi} \gamma_5 \gamma^{\{\sigma} D_1^\mu \dots D_1^{\mu_{n-1}}\}} \lambda_i \psi | p s \rangle \quad (2.4)$$

$$M d_n s^{\{\sigma p^{\mu_1} \dots p^{\mu_{n-1}}\}} = \langle p, s | i^{n-1} \bar{\psi} \gamma_5 \gamma^{\{[\sigma} D_1^{\mu_1]} \dots D_1^{\mu_{n-1}}\}} \lambda_i \psi | p s \rangle, \quad (2.5)$$

where  $\{\}$  denotes complete symmetrization. Notice that, even though the operators Eq. (2.2) are twist-2 and the operators Eq. (2.3) are twist-3, their respective contributions to the light-cone expansion of  $W^{\mu\nu}$  are of the same order in  $Q^2$ . In the singlet case, these operators will further mix with gluonic ones;<sup>\*16</sup> however, the first moment of  $g_1$ , which we will be mostly concerned with, is still given by Eq. (2.4).

The reason why we will concentrate our discussion on  $g_1$  is that for longitudinally polarized protons the only nonvanishing components of the hadronic tensor are<sup>14</sup> (in the frame where, say, only the third spatial component of  $q$  is nonzero and its energy vanishes)

$$W_A^{12} = -W_A^{21} = \pm \left[ g_1 - \left( \frac{2Mx}{Q} \right)^2 g_2 \right], \quad (2.6)$$

---

\* Note also that Eq. (2.5) is true only for strictly massless quarks; in general the operators contributing to  $g_2$  will mix with twist-3 mass dependent operators. The contribution of these operators does not vanish asymptotically, even though their matrix elements should be of order  $m/M$ , with  $m$  and  $M$  the quark and nucleon masses.

hence only  $g_1$  is relevant asymptotically. For transverse polarization (along, say, the first spatial coordinate) the nonvanishing components are instead

$$W_A^{02} = -W_A^{20} = \frac{2Mx}{Q} [g_1 + g_2], \quad (2.7)$$

thus, even though the two structure functions contribute equally to it, the whole cross section vanishes asymptotically. Only an experimental upper bound on  $g_2$  is thus presently available;<sup>17</sup> an alternative determination of it is forthcoming.<sup>6</sup>

In general,  $\Gamma_1$  will receive both singlet and nonsinglet contributions, and it is therefore convenient to define axial charges  $a_i$  for the  $i$ -th flavor:

$$Ma_i s^\mu \equiv \langle p, s | \bar{\psi}_i \gamma_\mu \gamma_5 \psi_i | p, s \rangle. \quad (2.8)$$

The first moment of  $g_1$  [Eq. (1.1)] for a nucleon target is then given by

$$\begin{aligned} \Gamma_1^{p,n}(Q^2) &= \frac{1}{2} \left[ \sum_{i=1}^{N_f} e_i^2 C_i(Q^2) a_i \right] \\ &= \frac{1}{12} \left[ C_{NS}(Q^2) \left[ \pm (a_u - a_d) + \frac{1}{3} (a_u + a_d - 2a_s) \right] + C_S(Q^2) \frac{4}{3} (a_u + a_d + a_s) \right], \end{aligned} \quad (2.9)$$

where in the last step we have assumed that only the three lightest flavors are activated, the plus (minus) sign refers to the proton (neutron), and the explicit form of the singlet and nonsinglet coefficient functions  $C_S$ ,  $C_{NS}$  will be given in Sect. 3.2.

### 3. Phenomenology of $g_1^p$

The primary quantity from which experimental information on polarized structure functions is obtained is the polarization asymmetry  $A(x, Q^2) = \frac{\sigma^{\uparrow\uparrow} - \sigma^{\uparrow\downarrow}}{\sigma^{\uparrow\uparrow} + \sigma^{\uparrow\downarrow}}$ . In order to relate this to  $W^{\mu\nu}$  [Eq. (2.1)], we must extract from  $A$  the asymmetry for scattering of transverse (*i.e.* with longitudinal helicity) virtual photons, defined as

$$A_1(x, Q^2) = \frac{\sigma_{1/2} - \sigma_{3/2}}{\sigma_{1/2} + \sigma_{3/2}} \quad (3.1)$$

where the subscripts denote the total angular momentum of the photon-nucleon pair along the incoming electron's direction; the denominator of (3.1) is the total transverse photoabsorption cross section  $\sigma_T = \sigma_{1/2} + \sigma_{3/2}$ .  $A$  is related to  $A_1$  by  $A = D(A_1 + \eta A_2)$ , in terms of the factor  $D$  which provides the longitudinal depolarization of the virtual photon with respect to its parent lepton, the interference  $A_2$  with the longitudinal photon polarization amplitude, and a kinematic factor  $\eta$ .

The asymmetry  $A_1$  measures the ratio between the combination (2.1) of polarized structure functions, and the unpolarized structure function  $F_1$  (the other independent unpolarized structure function gives the total longitudinal cross section). In the Bjorken limit the contribution of  $g_2$  is negligible [Eq. (2.6)] only  $g_1$  contributes to the numerator in Eq. (3.1), and  $g_1$  is given by

$$g_1(x, Q^2) = A_1(x, Q^2)F_1(x, Q^2) \quad (3.2)$$

$$= A_1(x, Q^2) \frac{F_2(x, Q^2)}{2x [1 + R(x, Q^2)]}, \quad (3.3)$$

where the last step holds at leading twist. The unpolarized structure function  $F_2$  is directly determined from experiment, and has the simple parton model interpretation (which in the DIS scheme remains true to all orders in perturbative QCD)

$$\frac{F_2(x)}{x} = \sum_{i=1}^{N_f} e_i^2 [q_i(x) + \bar{q}_i(x)], \quad (3.4)$$

while  $R = \frac{\sigma_L}{\sigma_T}$ , where  $\sigma_L$  is the longitudinal virtual photoabsorption cross section. Because in the Bjorken limit  $R$  vanishes, Eq. (3.4) reduces to  $g_1 \approx A_1 F_2 / (2x)$ ; in particular, in the naive parton model it thus follows that

$$g_1^{\text{parton}}(x) = \sum_{i=1}^{N_f} e_i^2 [\Delta q_i(x) + \Delta \bar{q}_i(x)], \quad (3.5)$$

where  $\Delta q_i$  are the polarized parton distributions for quarks of flavor  $i$ .

A precise determination of  $g_1$  thus hinges on the following assumptions. First,  $A_1$  must be determined from the measured asymmetry  $A$ : in older experiments<sup>1,2</sup> this was done by simply neglecting  $A_2$  and identifying  $A$  with  $DA_1$ . Then, the contribution of  $g_2$  to  $A_1$  is neglected, exploiting Eq. (2.6), so that Eq. (3.2) holds. Finally,  $g_1$  is determined from the measured  $F_2$  using Eq. (3.3), the main uncertainty being in the experimental knowledge of  $R$ . The first assumption is under control:  $A_2$  satisfies a positivity limit  $|A_2| \leq \sqrt{R}$ , and is now<sup>17</sup> measured to be compatible with zero within uncertainties, so that (taking also advantage of the fact that the coefficient  $\eta$  turns out to be small in the kinematic range covered by present experiments) its possible effects are just included in the systematic error. The neglect of  $g_2$  should not affect the determination of the first moment of  $g_1$ , since, regardless of the size of  $g_2$ , its first moment is expected to vanish (according to the Burkhardt-Cottingham sum rule);<sup>12,18</sup> even if it did not (due to nonperturbative effects) its contribution is estimated<sup>19</sup> to modify the first moment of  $g_1$  by at most 1%. A precise measurement of  $g_2$  would settle the issue. The last step of the analysis is also under complete control: due to cancellations in the dependence of  $D$  and  $F_1$  on  $R$ , the asymmetry  $g_1$  is in fact essentially independent of  $R$ .<sup>4</sup> All these effects combined lead thus to an uncertainty of a few per cent, which is included in the experimental error and is smaller than the uncertainty on the unpolarized structure function  $F_2$ .

In the remainder of this section, we will consider in particular the proton experiments, which afford the best experimental accuracy.

### 3.1. Scale dependence and $x$ -extrapolation

The values of  $g_1$  which can be determined using Eq. (3.3) span in practice a limited kinematic range: very small and large  $x$  regions are excluded, while low  $x$  data are taken at low  $Q^2$  and conversely. Thus, in order to obtain a determination of  $g_1(x, Q^2)$  for all  $x$  and one single value of  $Q^2$ , the data must be evolved to a common  $Q^2$  and then extrapolated over the whole  $x$  range.

The scale dependence of the asymmetry  $A_1$  is given by the Altarelli-Parisi equations, and follows from the fact that  $g_1$  and  $F_2$  depend on  $Q^2$  in different ways, even at leading order. This is apparent if one considers the respective first moments: at one loop the anomalous dimension of  $\Gamma_1$  vanishes (the axial current is classically conserved; this conservation is spoiled by the axial anomaly, but this is a two-loop effect), while the first moment of  $F_2$  evolves since obviously the total number of  $q$ - $\bar{q}$  pairs is not conserved. The scale dependence is thus calculable, the only theoretical uncertainty being that related to the relatively poor knowledge of polarized parton distributions (see Sect. 4.2). The result of the calculation,<sup>20</sup> with two extreme scenarios for the polarized gluon distribution, is displayed and compared with the data of Ref. 1 in Fig. 2a.

Clearly, the data are not precise enough to display the calculated scale dependence, even though they are consistent with it (the same applies to more recent data<sup>3</sup>), which explains why the scale dependence of the asymmetry is not yet observed directly. Nevertheless, the average scale of the smallest and largest  $x$  bins is often rather different: for example in Ref. 4 the smallest  $x$  bin ( $\langle x \rangle = 0.005$ ) has  $\langle Q^2 \rangle = 1.3 \text{ GeV}^2$ , and the largest  $x$  bin ( $\langle x \rangle = 0.48$ ) has  $\langle Q^2 \rangle = 58.0 \text{ GeV}^2$ . It is therefore important to correct the data for this effect, *i.e.* to evolve the measured asymmetry to the common scale at which  $g_1$  is to be determined. The size of the correction (shown in Fig. 2b for the data of Ref. 2) depends strongly on this scale: the correction on  $\Gamma_1^p$  is smaller than 5% for the determination of Ref. 2, which is given at  $Q^2 = 10.7 \text{ GeV}^2$ , but is for instance of order 10% for the deuteron data<sup>22</sup> at  $Q^2 = 4.7 \text{ GeV}^2$ . The overall effect is anyhow larger than the uncertainty involved in its determination (which is mostly due to the uncertainty in the form of the polarized gluon distribution) and should therefore be included in the analysis of the data, especially if  $g_1$  is to be determined at low ( $Q^2 \lesssim 5 \text{ GeV}^2$ ) scales.

Once the data are evolved to a common scale,  $g_1$  is still only known over a limited  $x$  range: for example, the combined data of Refs. 21 and 2 have  $0.01 \leq x \leq 0.7$ , and the more recent ones of Ref. 4 have  $0.003 \leq x \leq 0.7$ . In order to be able to compute moments of  $g_1$ , which are the primary quantities in QCD,  $g_1$  thus has to be extrapolated at small and large  $x$ .

The large  $x$  behavior should be controlled by QCD counting rules:<sup>23,24</sup> because for large  $x$  the virtuality of the struck quark is large, the scattering process should be purely perturbative, and the dominant contribution to it should come from minimally connected tree graphs, *i.e.* those where three valence quarks exchange two perturbative gluons. This leads to the prediction

$$G_q \sim (1-x)^p; \quad p = 2n - 1 + 2\Delta s_z, \quad (3.6)$$

where  $G_q$  is any parton distribution,  $n$  is the number of spectator quark lines (*i.e.*,  $n = 2$  for a nucleon) and  $\Delta s_z = 0$  ( $\Delta s_z = 1$ ) for parallel (antiparallel) quark and proton helicities. This implies that in the approximation of Eq. (3.5) one would expect

$$A_1 \underset{x \rightarrow 1}{\sim} \text{const.}; \quad g_1 \underset{x \rightarrow 1}{\sim} (x - 1)^3. \quad (3.7)$$

The fall-off of  $g_1$  at large  $x$  implies that the contribution of the large  $x$  extrapolation to  $\Gamma_1$  is expected to be small, *i.e.* around a few per cent of  $\Gamma_1$ . The extrapolation has been performed by fitting a phenomenological function either to  $A_1$  (which amounts to fitting a straight line through the last few data points),<sup>2</sup> or to  $g_1$ .<sup>5</sup> The (preliminary) result of the latter extrapolation actually turns out to be surprisingly large (by a factor 3 larger than that of Ref. 4); this appears to be due to an actual difference in the data, and not to the method used in the extrapolation; however, the large  $x$  points have large uncertainties — indeed all experiments are compatible with each other — and the effect on  $\Gamma_1$  is anyway modest. The same applies to results obtained<sup>24</sup> by imposing the behavior Eq. (3.6). A different estimate has also been obtained by using a valence quark model,<sup>9</sup> which is consistent with the behavior (3.6) but predicts also its normalization; the results are similar (see however the discussion of the deuterium data in Sect. 5).

The small- $x$  extrapolation is somewhat harder to control. Arguments based on the dominance of known Regge poles<sup>25</sup> lead to the expectation

$$g_1 \underset{x \rightarrow 0}{\sim} x^\alpha; \quad 0 \leq \alpha \leq 0.5. \quad (3.8)$$

However, use of perturbative QCD together with an Ansatz for the nucleon wave function<sup>24</sup> suggests that the gluon distribution should behave as

$$\frac{\Delta G_q}{G} \underset{x \rightarrow 0}{\sim} x; \quad (3.9)$$

thus, if the unpolarized gluon distribution is dominated by a soft pomeron,<sup>26</sup> then  $G(x) \sim \frac{1}{x}$  so that the lower bound for  $\alpha$  in Eq. (3.8) is saturated; but if  $G(x)$  has a harder behavior (such as a supercritical or perturbative pomeron<sup>26</sup>) then  $\alpha < 0$  ( $\alpha \sim -0.1$  with a supercritical pomeron, and even lower with the Lipatov hard pomeron<sup>26</sup>). Due to QCD evolution the gluon feeds into the quark at small  $x$  (the eigenvector of the evolution being a linear combination of  $\Delta q$  and  $\Delta g$ ), and a singular behavior with the same value of  $\alpha$  is then induced in  $g_1$ .<sup>27</sup> Also, a model of the pomeron based on nonperturbative gluon exchange<sup>28</sup> leads to the still singular but softer behavior

$$g_1 \underset{x \rightarrow 0}{\sim} -2 \ln x. \quad (3.10)$$

Finally, it has been argued<sup>29</sup> that negative signature cuts could induce an even more singular behavior

$$g_1 \underset{x \rightarrow 0}{\sim} \frac{1}{x \ln^2 x}, \quad (3.11)$$



even though there is no compelling theoretical evidence in favor of such contributions. It is worth noticing that not all these behaviors are stable upon perturbative evolution:<sup>27</sup> in general if, at some scale  $Q_0$ ,  $g_1$  is regular, or has a singularity of the form (3.8) with  $\alpha \lesssim 0.1$  or softer [such as (3.10)], then at larger  $Q$  and small  $x$ , due to QCD evolution, it will develop a double logarithmic singularity<sup>30</sup>

$$g_1 \underset{x \rightarrow 0}{\sim} \exp 2\gamma \sqrt{\log 1/x \log \log Q^2}; \quad \gamma^2 = (16/33 - 2n_f)[5 + 4\sqrt{1 - 3n_f/32}]. \quad (3.12)$$

More singular behaviors such as (3.11) will instead be preserved by the evolution. The issue is further complicated by the mixing of quark and gluon contributions, which turn out to contribute to the small- $x$  eigenvector with opposite signs.<sup>27</sup>

Keeping in mind that the theoretical picture is somewhat blurred, let us turn to the data. The earlier experiment,<sup>1</sup> which extends down to  $x = 0.015$ , fitted to the *asymmetry* a parametrization that behaves at small  $x$  as  $A_1 \underset{x \rightarrow 0}{\sim} x^{1.12}$  which then, assuming  $F_2 \underset{x \rightarrow 0}{\sim} \text{const.}$ , leads, by Eq. (3.3), to the behavior (3.8) with  $\alpha = 0.12$ . A direct fit of the form (3.8) to the last seven data points<sup>31</sup> leads to  $\alpha = 0.07_{-0.42}^{+0.32}$ . Finally, a recent determination<sup>32</sup> of  $F_2$  displays a fitted behavior  $F_2 \underset{x \rightarrow 0}{\sim} x^{-1.1}$ , which, if used together with the above parametrization of  $A_1$ , would lead to<sup>9</sup>  $\alpha = 0.02$ ; however if  $g_1$  is determined<sup>3</sup> from the measured asymmetry<sup>1</sup> using this form of  $F_2$ , the result can be still fitted with the function (3.8). Quantitatively, these methods all lead to a contribution to the first moment from the  $x < 0.01$  region

$$\Gamma_1^{\text{small } x} \equiv \int_0^{0.01} dx g_1(x) \approx 0.002, \quad (3.13)$$

which is about 2% of  $\Gamma_1$  (and usually just included in the systematic error on the value of  $\Gamma_1$ ).

The more recent experimental data,<sup>4</sup> however, extend to significantly smaller  $x$  ( $x_{\min} = 0.003$ ), and lead to the striking result displayed in Fig. 3: not only there is no evidence of a fall-off with  $x$ , but actually (even though with large errors) the last four data points display a rise at small  $x$ . These data have been extrapolated by fitting a constant value for  $g_1(x)$  to the last two points; the resulting contribution from the unmeasured small  $x$  region to  $\Gamma_1$  is now larger than in Ref. 2 by a factor 2, and adding to that the contribution from the (now measured)  $0.003 \leq x \leq 0.01$  range leads to a value of  $\Gamma_1^{\text{small } x}$  larger than Eq. (3.13) by a factor 6 or 7. Fitting the behavior (3.10) leads<sup>29</sup> to a similar result, while the very singular form of Eq. (3.11) gives a value which is yet larger by a factor 3, *i.e.*, about 20 times larger than Eq. (3.13). This alone would increase<sup>29</sup> the value of  $\Gamma_1$  by almost 25%.

Of course such conclusions should be taken with caution, especially since what is actually observed experimentally is an approximately constant behavior of the asymmetry  $A_1$ , and the rise is then produced by extrapolating a parametrization to  $F_2$  outside its declared<sup>32</sup> range of validity; furthermore, perturbative evolution may

substantially affect the small  $x$  behavior<sup>27</sup> and it is unclear that a small  $x$  tail fitted at  $\langle Q^2 \rangle \sim 1 \text{ GeV}^2$  can be assumed to be unchanged at  $\langle Q^2 \rangle = 10.7 \text{ GeV}^2$  where  $g_1(x)$  is given. Unfortunately the very recent SLAC data,<sup>5</sup> which have better statistics, only extend down to  $x_{\min} = 0.029$ ; they are consistent with the EMC/SMC data and, if fitted to a constant,<sup>6</sup> lead to a value of  $\Gamma_1^{\text{small } x}$  of the same size as that of Eq. (3.13).

### 3.2. Determining $\Delta\Sigma$

The singlet and nonsinglet components of  $\Gamma_1$  can be extracted using Eq. (2.9). This requires the determination of the matrix element of the triplet and octet current, and the computation of the coefficient functions  $C(Q^2)$ .

The triplet and octet current are conserved and therefore scale independent; they can thus be taken from any other process. The triplet matrix element is accurately known, because (through trivial isospin algebra) it is equal to the axial coupling measured in nucleon  $\beta$ -decay:

$$a_u - a_d = \frac{G_A}{G_V} = F + D = 1.2573 \pm 0.0028, \quad (3.14)$$

where  $F$  and  $D$  are octet meson decay constants in the standard SU(3) parametrization. The octet matrix element is then given, using SU(3) symmetry, by

$$a_u + a_d - 2a_s = 3F - D = 0.579 \pm 0.025. \quad (3.15)$$

The value in Eq. (3.15) is obtained from the most recent fit<sup>29</sup> to octet decays; notice that these values are significantly different (and more precise) than those used in older analyses.<sup>2</sup>

Now,  $\Delta\Sigma$  is found rewriting Eq. (2.9) as

$$C_s(Q^2)\Delta\Sigma(Q^2) = 9\Gamma_1^p - \frac{C_{NS}(Q^2)}{2} (3F + D). \quad (3.16)$$

The two terms on the r.h.s. of Eq. (3.16) are roughly of the same size (typically,  $\Gamma_1 \sim 0.1$ ), thus  $\Delta\Sigma$  arises from a large cancellation between them. In the most recent and accurate data<sup>4</sup> the error on  $\Gamma_1$  is of order 10%, hence it still dominates over the error on  $3F + D$ , which is of order 1%.

Knowledge of the perturbative coefficient functions in Eq. (3.16) has considerably improved recently. The one-loop results have long been known, in both the nonsinglet<sup>15</sup> and singlet<sup>16</sup> cases; the nonsinglet two loop<sup>33</sup> and three loop<sup>34</sup> coefficients have been determined subsequently; the singlet two loop coefficient was recently calculated,<sup>35,36</sup> and estimates for the next corrections (*i.e.* three loop in

the singlet case, and four loop in the nonsinglet) have also been proposed.<sup>37</sup> The full results (in the  $\overline{\text{MS}}$  scheme) are

$$C_{NS}(Q^2) = \left[ 1 - \left(\frac{\alpha_s}{\pi}\right) - 3.5833 \left(\frac{\alpha_s}{\pi}\right)^2 - 20.2153 \left(\frac{\alpha_s}{\pi}\right)^3 - (\sim 130) \left(\frac{\alpha_s}{\pi}\right)^4 + \dots \right] \quad (3.17)$$

$$C_S(Q^2) = \left[ 1 - \left(\frac{\alpha_s}{\pi}\right) - 1.0959 \left(\frac{\alpha_s}{\pi}\right)^2 - (\sim 3.7) \left(\frac{\alpha_s}{\pi}\right)^3 + \dots \right], \quad (3.18)$$

where  $\sim$  denotes the estimated coefficients. The estimates are arrived at by requiring minimal scale sensitivity (plus, in the nonsinglet case, some guesswork), and should be taken with care. Two comments are in order here: first, higher loop corrections turn out to have relatively large coefficients and are not negligible if  $Q^2 \lesssim 5 \text{ GeV}^2$ ; also, all loop corrections go in the same direction, namely, for given  $\Gamma_1$  the value of  $\Delta\Sigma$  obtained from Eq. (3.16) increases as more perturbative orders are included. The overall effect of these corrections is of order 20% around  $Q^2 \sim 5 \text{ GeV}^2$ ; this is large enough for the uncertainty on  $\Lambda_{\text{QCD}}$  to reflect on an uncertainty on  $\Delta\Sigma$  of a few per cent. This sensitivity can be actually used to measure  $\alpha_s$  (see Sect. 6).

The scale dependence of the quantity on the l.h.s. of Eq. (3.16) is still not entirely specified, because the singlet matrix element  $\Delta\Sigma$  depends on  $Q^2$  (due to the anomalous nonconservation of the singlet axial current). Its scale dependence starts at next to leading order; the first two nontrivial coefficients have been computed,<sup>16,36</sup> while the next order is estimated<sup>37</sup>:

$$\Delta\Sigma(Q^2) = \left[ 1 + \frac{2}{3} \left(\frac{\alpha_s}{\pi}\right) + 1.2130 \left(\frac{\alpha_s}{\pi}\right)^2 + (\sim 3.6) \left(\frac{\alpha_s}{\pi}\right)^3 + \dots \right] \Delta\Sigma(\infty). \quad (3.19)$$

#### 4. The proton experimental results and their meaning

The current experimental knowledge on  $\Gamma_1$  and  $\Delta\Sigma$  for the proton is summarized in Table 1; the last column gives the proton matrix element of the strange axial current, and thus provides a measure of the Zweig rule violation in this channel. The first two rows of the column are obtained from the same raw data; the more recent value<sup>3</sup> of  $\Delta\Sigma$  differs essentially because of the use of updated values of  $F$  and  $D$  and the inclusion of higher loop corrections (the latter, however, have a negligible effect at this scale). The values of  $\Delta\Sigma$  shown in the table are as given by the respective references, except the value for the SLAC experiment,<sup>5</sup> which we determined using Eqs. (3.16) with the coefficient functions (3.17)-(3.18) and the decay constants (3.14)-(3.15). As more data become available, however, it is now

Ref.	$\langle Q^2 \rangle$	$\Gamma_1^p$	$\Delta\Sigma$	$a_s$
2, 21	10.7	$0.126 \pm 0.018$	$0.12 \pm 0.17$	$-0.19 \pm 0.06$
3	10.7	$0.126 \pm 0.018$	$0.14 \pm 0.17$	$-0.15 \pm 0.06$
4, 21	10.0	$0.142 \pm 0.014$	$0.27 \pm 0.13$	$-0.10 \pm 0.05$
5	3.0	$0.129 \pm 0.011$	$0.28 \pm 0.11$	$-0.10 \pm 0.04$

Table 1: Summary of proton experimental results. All results hold at the given scale.

more sensible to perform a global fit of  $\Delta\Sigma$  from the determinations of  $\Gamma_1$  in various experiments;<sup>11</sup> we will discuss this in Sect. 6.

All data points turn out to agree within errors; the SMC result<sup>4</sup> is substantially larger because of the unexpectedly large values of  $g_1$  in the small  $x$  region, which is not covered by other experiments. The recent, more precise (but still preliminary) SLAC data<sup>5</sup> also agree with previous data; the difference in value of  $\Gamma_1$  is mostly accounted for by  $Q^2$  evolution. The error on  $\Delta\Sigma$  is dominated by the uncertainty on  $\Gamma_1$ ; this, in turn, comes in roughly equal proportions from statistics and systematics in the EMC/SMC experiments, whereas it is systematics-dominated in the E143 experiment,<sup>5</sup> which has better statistics but a smaller kinematic coverage. If the large values of  $g_1$  at small  $x$  of Ref. 4 are confirmed, then the small- $x$  extrapolation of Ref. 5 will have to be corrected, since the effect on  $\Gamma_1$  is then comparable to the total uncertainty.

#### 4.1. Theoretical interpretation

The large violation of the Zweig rule displayed by the data of Table 1 has been variously dubbed “spin crisis” or “spin puzzle”. Why this result should be puzzling at all (after all the Zweig rule is only a phenomenological expectation, known to fail in some channels) is perhaps best understood from the point of view of someone who wishes to construct a parametrization of the polarized quark distributions  $\Delta q_i$  and gluon distribution  $\Delta G$ . In leading order,  $\Delta\Sigma$  is scale independent; also, in the parton model [Eq. (3.5)]  $\Delta\Sigma$  is just the fraction of the nucleon helicity carried by quarks. Parton model results are modified by QCD evolution, but since the first moment does not evolve this identification is retained. This is in keeping with the observation that [Eq. (1.3)]  $\Delta\Sigma$  is the coefficient of proportionality between the nucleon helicity and the quark axial charge, which coincides with the quark helicity for free, massless quarks. Thus,  $\Delta\Sigma$  is the normalization of the polarized parton distribution which is input to the perturbative evolution, and one would guess that it should just be equal to the spin fraction carried by quarks in quark models of the nucleon, which is typically<sup>7</sup>  $\sim 0.6 \pm 0.1$ ; hence the puzzle. Of course, this is a puzzle for parton models and parametrizations, but not for QCD, even less so for effective models of the nucleon.

The resolution of this difficulty in the parton model<sup>38</sup> is easy to state, and becomes apparent when the QCD evolution equations are solved in next to leading

order. The eigenvector of the QCD evolution equation for the first moment turns out to be

$$\Delta\Sigma = \sum_i \int_0^1 dx \Delta\tilde{q}_i = \sum_i \int_0^1 dx \left( \Delta q_i - \frac{\alpha_s}{2\pi} \Delta g \right) \quad (4.1)$$

whose anomalous dimension is equal to that of the axial current Eq. (3.19) (the eigenvector remains Eq. (4.1) even at higher orders). Now, the crucial point is that this anomalous dimension starts at next to leading order, which means that at leading order the combination  $\frac{\alpha_s}{2\pi} \Delta g$  is scale invariant; thus, the gluon contribution to Eq. (4.1) is not asymptotically suppressed by a power of  $\alpha_s$ , and the next to leading order analysis tells us that the one loop scale invariant combination which in the parton model is associated to  $\Delta\Sigma$  is that given in Eq. (4.1), and not the naive parton model one of Eq. (3.5). The polarized gluon distribution whose first moment appears in Eq. (4.1) is uniquely defined and can be independently measured in different hard processes,<sup>39,40</sup> even though in polarized deep-inelastic scattering it is only the combination in Eq. (4.1) which is measurable. It appears that the coefficient of the gluon contribution to Eq. (4.1) can be changed by using different regularizations of infrared collinear singularities,<sup>41</sup> thus modifying the amount of mixing between quarks and gluons, but a detailed analysis<sup>42</sup> shows that this can only be done by including soft contributions in a hard coefficient function. This said, the gluon coefficient in Eq. (4.1) can still be modified by reabsorbing the gluon contribution in a redefinition of the polarized quark distribution, *i.e.* by a change of scheme; however, the definition Eq. (4.1) is the unique one where  $\sum_i \Delta q_i$  is conserved to all orders, as the quark helicity must be.

The reason for these results resides in the anomalous conservation law satisfied by the axial current

$$\partial_\mu j_5^\mu = N_f \frac{\alpha_s}{2\pi} \text{tr} \epsilon^{\mu\nu\rho\sigma} F_{\mu\nu} F_{\rho\sigma}, \quad (4.2)$$

which is exact nonperturbatively. Due to the anomaly, matrix elements of the axial current do not measure directly the quark helicity, but rather a combination of the quark helicity and an anomalous non-conserved contribution; the latter reduces perturbatively to the expression Eq. (4.1), but can also receive a nonperturbative contribution  $\Omega$ , which need not have a partonic interpretation, so that in general<sup>43</sup>

$$\Delta\Sigma = \sum_i \int dx \Delta\tilde{q}_i - N_f \Omega. \quad (4.3)$$

The anomalous contribution is due to the helicity generated by anomalous particle creation,<sup>43</sup> in analogy<sup>44</sup> to electroweak baryon number generation.\* In principle,

---

\* The fact that the gluon contribution can be absorbed in the quark one by a choice of scheme, but at the expense of losing the conservation of first moment of the polarized quark density, corresponds to the fact that the anomalous dimension of the axial current can be set to zero by a finite renormalization (because it starts at two loops), but the mixing of the axial currents with the

the perturbative anomalous contribution  $\Delta g$  can be measured directly<sup>10,11</sup>, while the nonperturbative one  $\Omega$  can be revealed in different processes;<sup>46</sup> the former is scale dependent, as discussed above, while the latter is not.

Regardless of whether it is  $\Delta g$  or a nonperturbative contribution  $\Omega$ , a large cancellation between the quark contribution and the anomalous gluon contribution to  $\Delta\Sigma$  must be invoked to explain its observed small value. This cancellation in turn can only be explained in terms of a nonperturbative mechanism. While effective models of the nucleon, such as the Skyrme,<sup>47,48</sup> bag,<sup>49</sup> or Nambu–Jona-Lasinio<sup>50</sup> models can easily be made to accommodate the observed values of  $\Delta\Sigma$ ,  $F$  and  $D$  (but at the expense of introducing extra free parameters<sup>†</sup>), in these models it is impossible to separate quark and gluon contributions to observed quantities. On the other hand, a cancellation between  $\Delta q$  and  $\Omega$  in Eq. (4.3) can be explicitly shown to take place due to instanton-like configurations in the QCD vacuum,<sup>51</sup> however it is hard to go beyond model calculations.

A rather different understanding of the small value of  $\Delta\Sigma$  is arrived at in  $t$ -channel approaches, where the nucleon matrix element of the axial current is computed coupling the current to composite operators that correspond to physical bound states, which then couple irreducibly to the nucleon. The small value of  $\Gamma_1$  is then due to a strong nonperturbatively induced scale dependence,<sup>52</sup> or to the smallness of the relevant bound state propagator, which can be expressed using an exact Ward identity in terms of the topological susceptibility of the vacuum,<sup>53</sup> and estimated using QCD sum rules,<sup>54</sup> with results in excellent agreement with experiment. These approaches, which rely only on the nonperturbative QCD dynamics, imply that the smallness of  $\Gamma_1$  depends on the structure of the axial current, and is unrelated to the specific target which is being considered;<sup>54</sup> their relation to the parton approach, however, is not immediate.

#### 4.2. Polarized parton parametrizations

The problem of constructing a parametrization of polarized parton distributions is actually not an academic one. Earlier proposals, based on the idea of relating polarized distributions to unpolarized ones through a dilution factor<sup>55</sup> lead necessarily to results in disagreement<sup>1</sup> with the data; however, once the anomalous gluon contribution Eq. (4.1) is taken into account, the data can be fitted phenomenologically without giving up the idea that polarized and unpolarized quark distributions

---

(gluonic) anomaly operator cannot be removed (being a one-loop effect), and the coefficient of the mixing (the strength of the anomaly) is fixed in a scheme independent way once the way in which  $\Delta q$  renormalizes is specified. Of course, gluons will also contribute to higher moments of  $g_1$ , but this contribution is entirely scheme-dependent; the pertinent coefficient functions are given within specific choices of scheme in Ref. 45.

<sup>†</sup> For instance, the pure Skyrme model in the  $N_f \rightarrow \infty$  limit predicts<sup>47</sup>  $\Delta\Sigma = 0$  and cannot fit  $F$  and  $D$  accurately, but can be made to fit all the data by introducing corrections in  $\frac{1}{N_f}$  such as those due to coupling to vector mesons.<sup>48</sup>

should have the same gross features, either within the same approach,<sup>56</sup> or by constructing a parametrization from scratch.<sup>57</sup> Of course the data can also be described without anomalous contribution but assuming a large amount of Zweig rule violation (which is absent in the unpolarized case).

As more data become available, however, it is now possible to construct polarized parton distributions which incorporate all the constraints from perturbative QCD [Eqs. (3.6), (3.9)] as well as the general constraint from Regge theory that the small  $x$  behavior be isosinglet.<sup>45</sup> Imposing the constraints at a starting scale of  $Q^2 = 4 \text{ GeV}^2$  the data can then be fitted rather accurately, consistently including the scale dependence at leading order, and imposing cuts to keep higher twist corrections under control. The fit can be performed assuming the polarized sea quark distributions to be entirely generated by perturbative evolution;  $\Delta G$  turns out to be largely unconstrained, and can be chosen to have different large  $x$  behaviors. If the gluon is assumed to behave as a constant at small  $x$ , then the fit to the proton data<sup>21,2,4</sup> favors a singular quark of the form Eq. (3.8) (which dominates  $g_1$  at small  $x$ ), with  $\alpha \approx -0.55 \pm 0.15$ . The neutron structure function can then be predicted, the data not being good enough to constrain it seriously. Eventually, it should be possible to test these parametrization directly: while  $\Delta G$  can be measured typically by photon-gluon fusion,<sup>10</sup>  $\Delta q$  can in principle be measured for sea and valence flavors separately, by tagging final state hadrons; preliminary results<sup>58</sup> are consistent with the results of the fit to the proton data.<sup>45</sup>

## 5. Polarized scattering on neutrons

A measurement of  $g_1^n$  provides the determination of an independent linear combination of polarized quark distributions. Thus, neutron experiments, besides giving independent theoretical information on  $\Delta\Sigma$ , also offer the possibility of measuring directly the nonsinglet polarized structure function  $g_1^p - g_1^n$ , whose first moment is just [from Eq. (2.9)]

$$\Gamma_1^p - \Gamma_1^n = \frac{1}{6} C_{NS}(Q^2)(a_u - a_d). \quad (5.1)$$

A comparison of the data with the known value of  $a_u - a_d$  [Eq. (3.14)] and the computed  $C_{NS}$  [Eq. (3.17)] thus allows a direct test of isospin in this channel, as well as of the predicted scale dependence. However, neutron experiments are somewhat subtler, both because nuclear effects have now to be taken into account, and because they generally have a more restricted kinematic coverage than proton experiments.

The neutron structure function can only be measured by scattering on nuclear targets. Specifically, deuterium<sup>22,5</sup> and  $^3\text{He}$  targets<sup>59</sup> have been used. In the former case, assuming additivity, one obtains a determination of  $g_1^p + g_1^n$ ; in the latter case, the two protons are mostly in an  $S$ -state so that the spin of the nucleus is carried by the neutron. In both cases, however, there are complications due to nuclear

structure. Taking into account that the deuteron can be in  $D$  wave with probability  $\omega_D$  one has<sup>22</sup>

$$\Gamma_1^p + \Gamma_1^n = \frac{2\Gamma_1^p}{1 - 1.5\omega_D}. \quad (5.2)$$

The  ${}^3\text{He}$  wave function has in general 10 components; a simplified description in terms of a three-component wave function leads to<sup>60</sup>

$$\Gamma_1^n = (1.15 \pm 0.02)\Gamma_1^{He} + (0.057 \pm 0.009)\Gamma_1^p, \quad (5.3)$$

which however only holds in the Bjorken limit, and could be significantly corrected at finite  $Q^2$ ; the error involved is still negligible compared to present day experimental accuracy. Further nuclear effects are due to Fermi motion (which for the deuteron is estimated<sup>61</sup> to lead to a sizable correction to  $g_1$ , up to perhaps 10%), and to shadowing and antishadowing.<sup>62</sup> No systematic investigation of the latter effects is available yet.

The problems related to  $Q^2$  evolution and  $x$  extrapolation discussed in Sect. 3.1 are even more serious in neutron experiments. An example is the uncertainty involved in the large  $x$  behavior of the deuterium data<sup>22</sup>: if this is determined assuming a valence quark model<sup>9</sup> at large  $x$ , rather than fitting the data directly, the value<sup>22</sup> of  $\Gamma_1^n$  increases by a factor two;<sup>9</sup> however, the data are sufficiently uncertain that the two results are still compatible within errors. The problems related to small  $x$  are shown in Fig. 4, which displays the extrapolation of the E142 data, performed assuming a Regge-like behavior  $A_1^n \underset{x \rightarrow 0}{\sim} x^{1.2}$ ,<sup>59</sup> compared with an extrapolation of neutron data obtained by combining the SMC data<sup>22</sup> with the EMC proton data,<sup>2</sup> and then fitting a power behavior Eq. (3.8) to the last data point. These two extrapolations lead to values of  $\Gamma_1^n$  which differ by over 30%.

The issue of scale dependence is particularly serious here because all neutron data are taken at very low  $Q^2$ . This not only means that the (calculable) effects of QCD evolution due to difference in scale between  $x$  bins are now rather sizable (the correction on the first moment is of order 10%),<sup>20</sup> but also, that higher twist effects can be important. If these effects are included, then, for instance, the scale dependence of the nonsinglet first moment in Eq. (5.1) is modified as

$$\Gamma_1^p - \Gamma_1^n = \frac{1}{6} \left[ C_{NS}(a_u - a_d) + \frac{c_{HT}}{Q^2} \right]. \quad (5.4)$$

The value of  $c_{HT}$  in Eq. (5.4) has been the subject of considerable controversy: QCD sum rules lead<sup>63</sup> to  $c_{HT} = -0.09 \pm 0.06$ , but a different estimate based on the same method<sup>64</sup> has  $c_{HT} = -0.15 \pm 0.02$ ; a bag model computation<sup>65</sup> even leads to a result with the opposite sign,  $c_{HT} = 0.16$ . The sum rule method appears to be self-consistent in that a different sum rule<sup>66</sup> leads essentially to the same result as Ref. 63; the theoretical uncertainty is perhaps of order 50%.<sup>66</sup> The scale dependence of the isotriplet  $\Gamma_1$  is displayed in Fig. 5; higher twist effects are included according



Ref.	$\langle Q^2 \rangle$	$\Gamma_1$	$\Delta\Sigma$	$a_s$
22	4.7	$\Gamma_1^d = 0.023 \pm 0.025$	$0.06 \pm 0.25$	$-0.21 \pm 0.08$
59	2.0	$\Gamma_1^n = -0.022 \pm 0.011$	$0.57 \pm 0.11$	$-0.01 \pm 0.06$
3	5.0	$\Gamma_1^n = -0.055 \pm 0.025$	$0.24 \pm 0.23$	$-0.11 \pm 0.08$
5	3.0	$\Gamma_1^d = 0.044 \pm 0.005$	$0.35 \pm 0.05$	$-0.08 \pm 0.03$

Table 2: Summary of neutron and deuteron experimental results. All results hold at the given scale;  $\Gamma_1^d \equiv (\Gamma_1^p + \Gamma_1^n)/2$

to Eq. (5.4) with  $c_{HT} = -0.1$ . This shows that the magnitude of higher twist correction is comparable to that of three loop corrections, but smaller than the uncertainty on  $\Lambda$ .

The neutron experiments are summarized in Table 2. The result of Ref. 3 (shown in Fig. 4) is obtained by putting together the neutron data of Ref. 59 with the values of  $g_1^n$  obtained combining  $g_1^p + g_1^n$  determined from the deuterium experiment<sup>59</sup> with proton data.<sup>2,21</sup> The values of  $\Delta\Sigma$  and  $a_s$  are as quoted by the respective references, except the entry corresponding to the preliminary result of Ref. 5, which we determined using the weak decay constants Eqs. (3.14)-(3.15), and the coefficient functions (3.17)-(3.18).

Again, all experiments agree within errors. The error on the SMC data<sup>22</sup> is mostly statistical, whereas the E142-E143 data,<sup>59,5</sup> which have generally better statistics (but smaller kinematic coverage), have approximately equal statistical and systematic uncertainty. The significantly larger values of  $\Gamma_1^n$  found by the SLAC experiments<sup>59,5</sup> appear to be mostly due to the small- $x$  region, as shown by the fact that the values of  $\Gamma_1^n$  of Refs. 59 and 3 differ essentially because of the contribution from this region (notice however that they are compatible within errors). If the trend displayed by the SMC data at small  $x$  (Fig. 4) is confirmed, the small  $x$  extrapolation of the more precise data<sup>5</sup> would have to be corrected accordingly.

## 6. Summary: the data and sum rules

The determinations of  $\Gamma_1$  with proton, neutron, and deuterium targets can now be compared with each other and with QCD expectations; the results, evolved to a common scale using the perturbative coefficient functions of Sect. 3.2 to highest available order (omitting higher order estimates and higher twist corrections), are displayed in Fig. 6.

First, the isotriplet first moment can be checked against the prediction of Eq. (5.1) (Bjorken sum rule<sup>67</sup>), thereby checking isospin in this channel. As is apparent from Fig. 6, the prediction is perfectly verified within current experimental errors, which means that it is verified to 10% accuracy. If, as the experimental precision improves, a violation of the sum rule within these bounds were found, it would not necessarily signal a breakdown of perturbative QCD: on the one hand,

it has been argued<sup>68</sup> that isospin breaking in meson-nucleon couplings could lead to a violation of the Bjorken sum rule up to 20%; also, the anomalous contribution  $\Omega$  [Eq. (4.3)] to the singlet matrix element  $\Delta\Sigma$ , due to its infrared sensitivity, could develop<sup>69</sup> a nonsinglet component (triggered by SU(2) violation in light quark masses) of up to 10%.

Then, a common value of  $\Delta\Sigma$  can be extracted. This is best done<sup>11</sup> by fitting the expression (2.9) to the data with fixed values of the weak decay constants, and  $\Delta\Sigma(Q^2 = \infty)$  left as a free parameter. The result, obtained from all the data of Tables 1 and 2 (excluding the entries corresponding to Ref. 3) is<sup>11</sup>

$$\Delta\Sigma(Q^2 = \infty) = 0.31 \pm 0.04. \quad (6.1)$$

This corresponds to  $a_s(Q^2 = \infty) = -0.097 \pm 0.018$ : the parton-based expectation that  $a_s$  should be compatible with zero (Ellis-Jaffe sum rule<sup>70</sup>) is thus violated by several standard deviations, with the theoretical implications discussed in Sect. 4.1.

Finally, the considerable scale sensitivity of the first moments (compare Fig. 5), especially in the  $Q^2 \lesssim 5 \text{ GeV}^2$  region, can be used to measure  $\alpha_s$ .<sup>71,11</sup> The simplest way of doing this is to take advantage of the fact that both the scale dependence and the normalization of the isotriplet combination in Eq. (5.1) are accurately predicted, so that comparing an experimental determination of  $\Gamma_1^p - \Gamma_1^n$  at finite  $Q^2$  to the asymptotic value Eq. (3.14) gives immediately a determination of  $\alpha_s$ . Including all known perturbative corrections and estimates of higher loops (but not higher twist corrections), and using  $\Gamma_1^n$  of Ref. 59 (as reanalysed in Ref. 8) and  $\Gamma_1^p$  of Ref. 5 gives<sup>71</sup>

$$\alpha_s(M_Z^2) = 0.122_{-0.009}^{+0.005}, \quad (6.2)$$

in good agreement with the current world average, and with surprisingly small error. This error, however, does not include the uncertainty related to the higher twist correction: if it is taken into account using Eq. (5.4) with  $c_{HT} = -0.12 \pm 0.06$  (according to the sum rule estimate discussed in Sect. 5), then<sup>71</sup>  $\alpha_s(M_Z^2) = 0.118_{-0.014}^{+0.007}$ . A determination which includes all the available information can be arrived at fitting Eq. (2.9) to all the available data, with both  $\Delta\Sigma$  and  $\alpha_s$  left as free parameters; the result is<sup>11</sup> (neglecting again higher twist effects)

$$\Delta\Sigma(Q^2 = \infty) = 0.33 \pm 0.04; \quad \alpha_s(M_Z^2) = 0.125 \pm 0.006. \quad (6.3)$$

This result is once more surprisingly accurate, and in good agreement with Eq. (6.2). It would be interesting to also fit simultaneously  $\alpha_s$ ,  $\Delta\Sigma$ , and the octet combination  $a_u + a_d - 2a_s$ , but current data are not accurate enough.<sup>71,11</sup>

In conclusion, combining all available results leads to a consistent picture, in excellent agreement with the predictions of perturbative QCD, and with interesting implications for the nucleon structure. While the improving quality of experimental data requires a more sophisticated theoretical analysis, it is now possible to test our understanding of several subtle perturbative QCD effects, and to start coping with the nonperturbative effects which determine the structure of the nucleon.

**Acknowledgements:** I wish to thank B. L. Ward for his warm hospitality in Tennessee; G. Altarelli and L. Stuart for discussions, R. Ball for a critical reading of the manuscript, F. Close and M. Einhorn for comments, and especially G. Ridolfi for considerable help in analysing the data.

## References

- [1] EMC Collaboration, J. Ashman et al., *Phys. Lett.* **B206** (1988) 364
- [2] EMC Collaboration, J. Ashman et al., *Nucl. Phys.* **B328** (1989) 1
- [3] SMC Collaboration, B. Adeva et al., *Phys. Lett.* **B320** (1994) 400
- [4] SMC Collaboration, D. Adams et al., *Phys. Lett.* **B329** (1994) 399
- [5] E143 Collaboration, R. Arnold et al., preliminary results presented at ICHEP94, Glasgow, August 1994
- [6] L. Stuart, these proceedings
- [7] R. L. Jaffe and A. Manohar, *Nucl. Phys.* **B337** (1990) 509
- [8] J. Ellis and M. Karliner, *Phys. Lett.* **B313** (1993) 131; talk at PANIC 1993, Perugia, July 1993, preprint CERN-TH.7022/93
- [9] F. Close and R. D. Roberts, *Phys. Lett.* **B316** (1993)165
- [10] G. Altarelli, in “The challenging questions”, Proc. of the 1989 Erice School, A. Zichichi, ed. (Plenum, New York, 1990)
- [11] G. Altarelli and G. Ridolfi, preprint CERN-TH.7415/94
- [12] R. L. Jaffe, *Comm. Nucl. Part. Phys.* **14** (1990) 239
- [13] R. L. Jaffe, in “Structure of baryons and related mesons”, Proc. of the Baryon’92 Conference, M. Gai, ed. (World Scientific, Singapore, 1993)
- [14] G. Altarelli, *Phys. Rep.* **81** (1982) 1
- [15] J. Kodaira et al., *Phys. Rev.* **D20** (1979) 627; *Nucl. Phys.* **B159** (1979) 99
- [16] J. Kodaira, *Nucl. Phys.* **B165** (1980)129
- [17] SMC Collaboration, D. Adams et al., *Phys. Lett.* **B336**, 125 (1994)
- [18] G. Altarelli, B. Lampe, P. Nason and G. Ridolfi, preprint CERN-TH.7254/94 (1994)
- [19] M. Anselmino and E. Leader, *Z. Phys.* **C41** (1988) 239
- [20] G. Altarelli, P. Nason and G. Ridolfi, *Phys. Lett.* **B320** (1994) 152
- [21] E80 Collaboration, M. J. Alguard et al., *Phys. Rev. Lett.* **37** (1976) 1261; **41** (1978) 70;  
E130 Collaboration, G. Baum et al., *Phys. Rev. Lett.* **51** (1983) 1135
- [22] SMC Collaboration, B. Adeva et al., *Phys. Lett.* **B302** (1993) 533
- [23] R. Blankenbecler and S. J. Brodsky, *Phys. Rev.* **D10** (1974) 2973; J. F. Gunion, *Phys. Rev.* **D10** (1974) 242
- [24] S. J. Brodsky, M. Burkardt and I. Schmidt, preprint SLAC-PUB-6087 (1994)
- [25] R. L. Heimann, *Nucl. Phys.* **B64** (1973) 429
- [26] See e.g. B. Badełek et al., *Rev. Mod. Phys.* **64**, 927 (1992)
- [27] R. D. Ball, S. Forte and G. Ridolfi, “Polarized structure functions at small  $x$ ”, *in preparation*

- [28] S. D. Bass and P. V. Landshoff, Cambridge preprint DAMTP 94/50
- [29] F. E. Close and R. G. Roberts, *Phys. Lett.* **B336** (1994) 257
- [30] M. A. Ahmed and G. G. Ross, *Phys. Lett.* **B56** (1975) 385;  
M. B. Einhorn and J. Soffer, *Nucl. Phys.* **B74** (1986) 714
- [31] J. Ellis and M. Karliner, *Phys. Lett.* **B213** (1988) 73
- [32] NMC Collaboration, P. Amaudruz et al., *Phys. Lett.* **B295** (1992) 159
- [33] S. G. Gorishny and S. A. Larin, *Phys. Lett.* **B172** (1986) 109
- [34] S. A. Larin and J. A. M. Vermaseren, *Phys. Lett.* **B259** (1991) 345
- [35] E. B. Zijlstra and W. L. van Neerven, *Nucl. Phys.* **B417** (1987) 452
- [36] S. A. Larin, *Phys. Lett.* **B334** (1994) 192
- [37] A. L. Kataev, preprint CERN-TH.7333/94 (1994)
- [38] G. Altarelli and G. G. Ross, *Phys. Lett.* **B212** (1988) 391
- [39] R. D. Carlitz, J. C. Collins and A. H. Muller, *Phys. Lett.* **B214** (1988) 229
- [40] G. Altarelli and B. Lampe, *Z. Phys.* **C47** (1990) 315
- [41] G. T. Bodwin and J. Qiu, *Phys. Rev.* **D41** (1990) 2755
- [42] W. Vogelsang, *Z. Phys.* **C50** (1991) 275
- [43] S. Forte, *Phys. Lett.* **B224** (1989) 189; *Nucl. Phys.* **B331** (1990) 1
- [44] B. Patel, Columbia University preprint CU-TP-599 (1993)
- [45] T. Gehrmann and W. J. Stirling, Durham preprint DTP/94/38 (1994)
- [46] M. Anselmino and S. Forte, *Phys. Rev. Lett.* **71** (1993) 223; *Phys. Lett.* **B323** (1994) 71
- [47] S. J. Brodsky, J. Ellis and M. Karliner, *Phys. Lett.* **B206** (1988) 309
- [48] R. Johnson et al., *Phys. Rev.* **D42** (1990) 2998;  
G. Kälbermann, J. M. Eisenberg and A. Schäfer, preprint hep-ph/9409299
- [49] B.-Y. Park et al., *Nucl. Phys.* **A504** (1989) 829
- [50] A. Blotz, M. Praszalowicz and K. Goetze, Bochum preprint RUB-TPII-41/93
- [51] S. Forte and E. V. Shuryak, *Nucl. Phys.* **B357** (1991) 153
- [52] R. D. Ball, *Phys. Lett.* **B266** (1991) 473
- [53] G. Shore and G. Veneziano, *Nucl. Phys.* **B381** (1992) 3
- [54] S. Narison, G. Shore and G. Veneziano, preprint CERN-TH.7223/94 (1994)
- [55] R. Carlitz and J. Kaur, *Phys. Rev. Lett.* **D38** (1977) 673
- [56] D. de Florian et al., *Phys. Lett.* **B319**, (1993) 285; preprint hep-ph/9408363
- [57] K. Sridhar and E. Leader, *Phys. Lett.* **B295** (1992) 283;  
J. Bartelski and S. Tatur, preprint hep-ph/9409204
- [58] SMC Collaboration, W. Wiślicki, preprint hep-ex/9405012
- [59] E142 Collaboration, P. L. Anthony et al., *Phys. Rev. Lett.* **71** (1993) 959
- [60] C. Ciofi degli Atti, E. Pace and G. Salmé, Istituto Superiore di Sanità (Rome)  
preprint INFN-ISS-93-3
- [61] M. V. Tokarev, *Phys. Lett.* **B318** (1994) 559
- [62] N. N. Nikolaev and V. I. Zakharov, *Phys. Lett.* **B55** (1975) 397;  
S. J. Brodsky and H. J. Lu, *Phys. Rev. Lett.* **64** (1990) 1342
- [63] I. I. Balitsky, V. M. Braun and A. V. Koleschnichenko, *Phys. Lett.* **B242** (1990)  
245; Erratum **B318** (1993) 648
- [64] G. G. Ross and R. G. Roberts, *Phys. Lett.* **B322** (1994) 425

- [65] X. Ji and P. Unrau, MIT preprint CTP-2232 (1993)
- [66] E. Stein et al., Frankfurt preprint UFTP 366/1994 (1994)
- [67] J. D. Bjorken, *Phys. Rev.* **148** (1966) 1467
- [68] I. Halperin, Tel Aviv preprint TAUP-2127-93 (1993)
- [69] S. Forte, *Phys. Lett.* **B309** (1993) 174
- [70] J. Ellis and R. L. Jaffe, *Phys. Rev.* **D9** (1974) 1444
- [71] J. Ellis and M. Karliner, preprint CERN-TH-7324/94 (1994)

## Figure Captions

- Fig. 1:** Experimental determinations of  $\Delta\Sigma^p$  (at the scale of the respective experiments, see Tab.1 below): a) cross, EMC (1988);<sup>1</sup>circle, EMC (1989);<sup>2</sup>diamond, world average (1994);<sup>3</sup>square, SMC (1994);<sup>4</sup>star, E142 (1994).<sup>5,6</sup> b) Theoretical reanalysis of the 1989 experiment<sup>2</sup>: cross, published value<sup>2</sup>; circle, Jaffe and Manohar (1990);<sup>7</sup>diamond, Ellis and Karliner (1993);<sup>8</sup>square, Close and Roberts (1993).<sup>9</sup>
- Fig. 2:** (from Ref. 20): a) Scale dependence of the asymmetry  $A_1(x, Q^2)$ , compared to the data. The crosses indicate data from Ref. 21 and the squares data from Ref. 2; the low (high) curves correspond to the lower (upper) edge of the  $x$ -bin, the solid (dashed) lines corresponds to a maximal polarized gluon (no polarized gluon). b) Effect on the data<sup>21,2</sup> of the scale dependence correction.
- Fig. 3:** a)(from Ref. 2) Experimental data for  $g_1^p(x)$  at  $\langle Q^2 \rangle = 10.7 \text{ GeV}^2$  (filled dots, EMC data;<sup>2</sup> open circles, SLAC data<sup>21</sup>); the dashed line is the small- $x$  extrapolation. b)(from Ref. 4) The data of Fig3a (here as triangles) compared to the new data.<sup>4</sup>
- Fig. 4:** (from Ref. 3) The E142<sup>59</sup> and SMC/EMC<sup>4,2</sup> data with the respective small  $x$  extrapolations (dashed: E142; solid: SMC/EMC)
- Fig. 5:** (adapted from Ref. 20) Scale dependence of the isotriplet first moment Eq. (5.1). Dashdot: tree-level result ( $C_{NS} = 1$ ); dotted: Leading order; dashed: three loops; solid: with higher twist. The three sets of curves correspond to the values  $\Lambda = 267, 383, 509 \text{ MeV}$ .
- Fig. 6:** Comparison of experimental determinations of  $\Gamma_1$  for proton,<sup>5</sup>neutron<sup>59</sup> and (dashed) deuteron.<sup>5</sup> The dotted lines indicate alternative proton<sup>2</sup> and neutron<sup>3</sup> determinations. The Bjorken sum rule prediction Eq. (5.1) is also shown (dot-dashed). All results have been evolved to  $Q^2 = 5 \text{ GeV}^2$ .

This figure "fig1-1.png" is available in "png" format from:

<http://arxiv.org/ps/hep-ph/9409416v2>

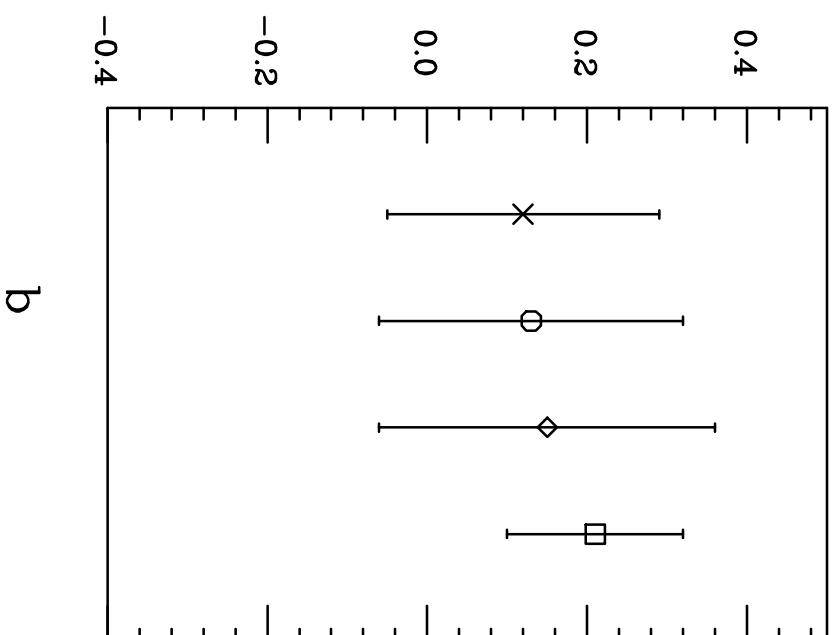
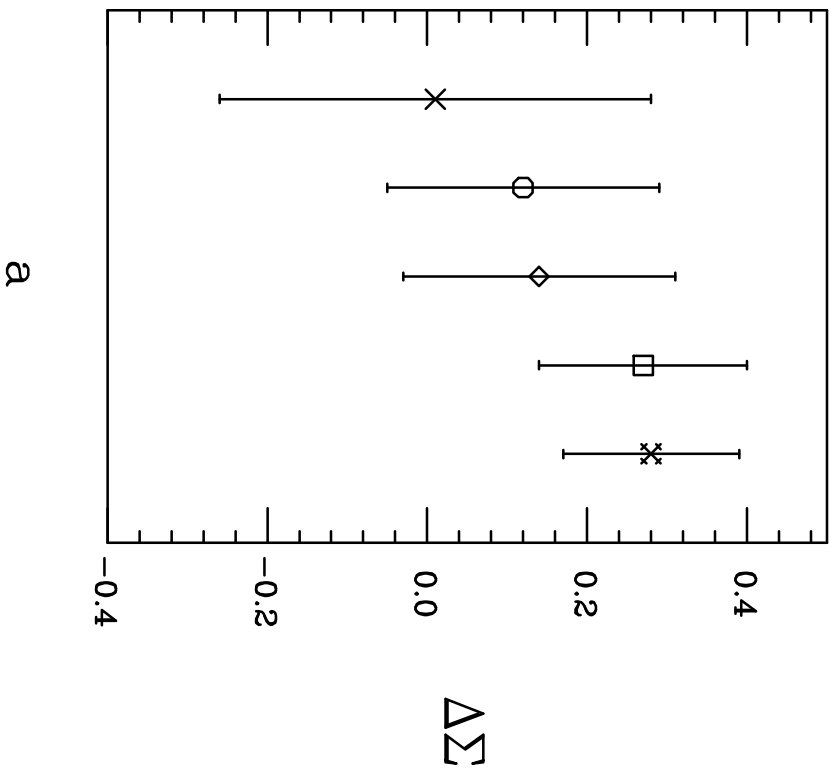
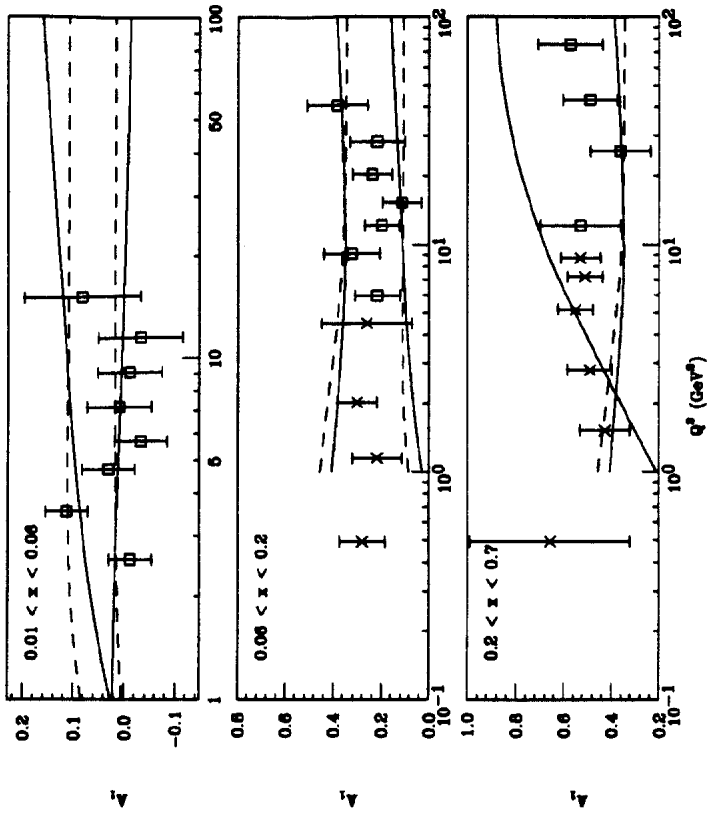


Fig. 1

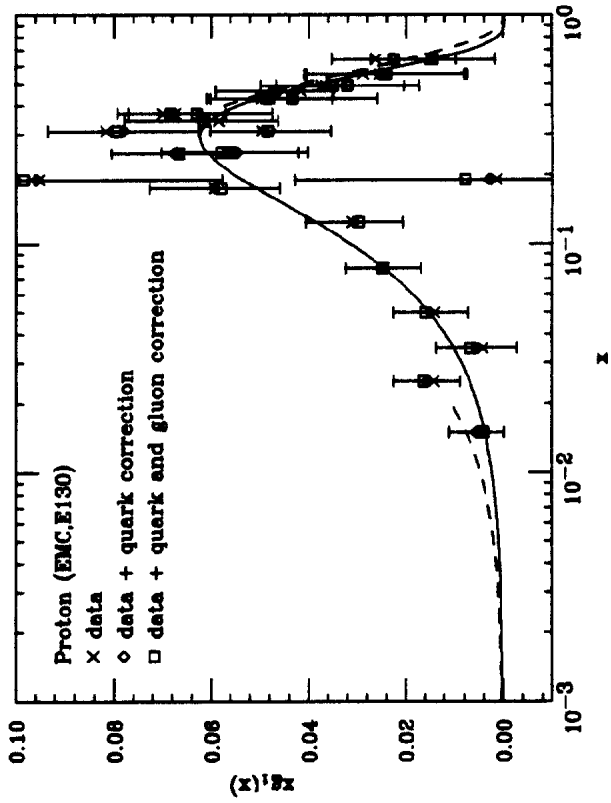


This figure "fig1-2.png" is available in "png" format from:

<http://arxiv.org/ps/hep-ph/9409416v2>



a

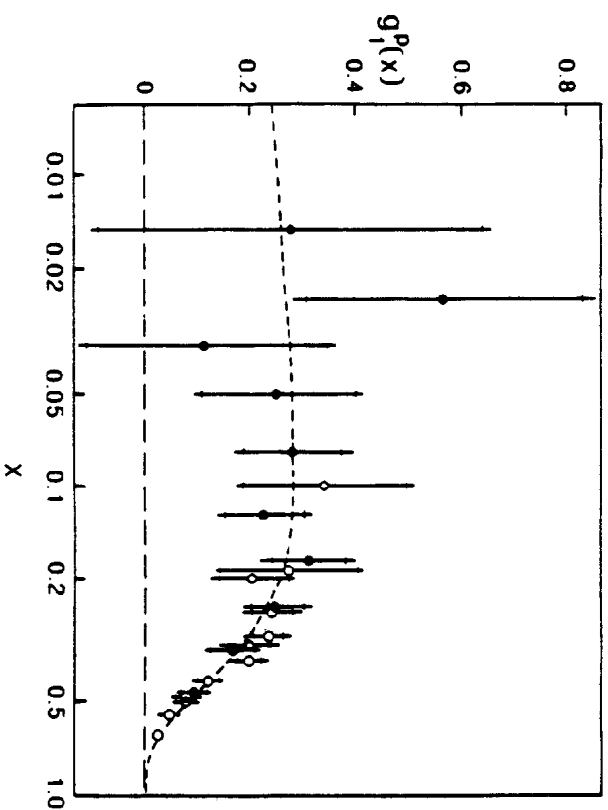


b

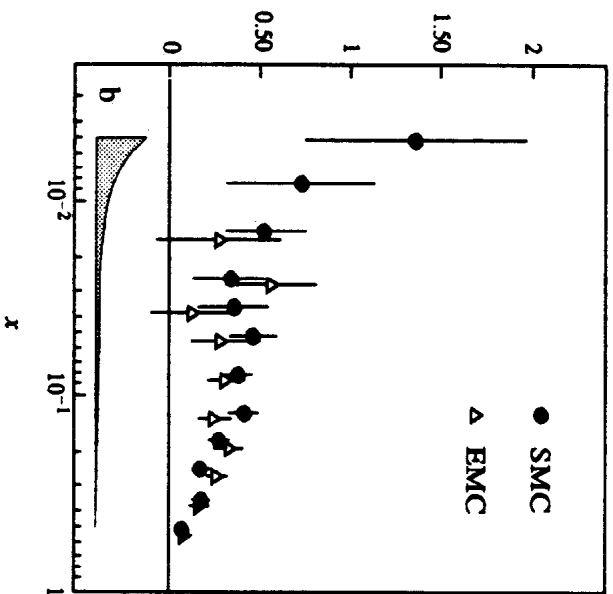
Fig. 2

This figure "fig1-3.png" is available in "png" format from:

<http://arxiv.org/ps/hep-ph/9409416v2>



a



b

Fig. 3

This figure "fig1-4.png" is available in "png" format from:

<http://arxiv.org/ps/hep-ph/9409416v2>

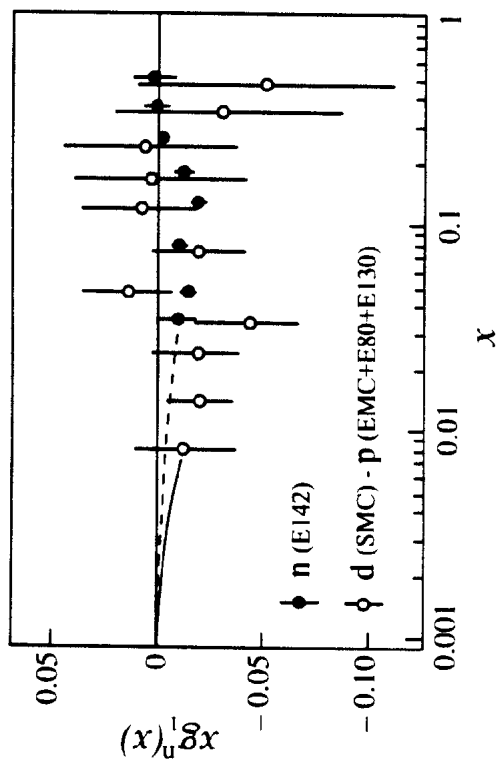


Fig. 4

This figure "fig1-5.png" is available in "png" format from:

<http://arxiv.org/ps/hep-ph/9409416v2>

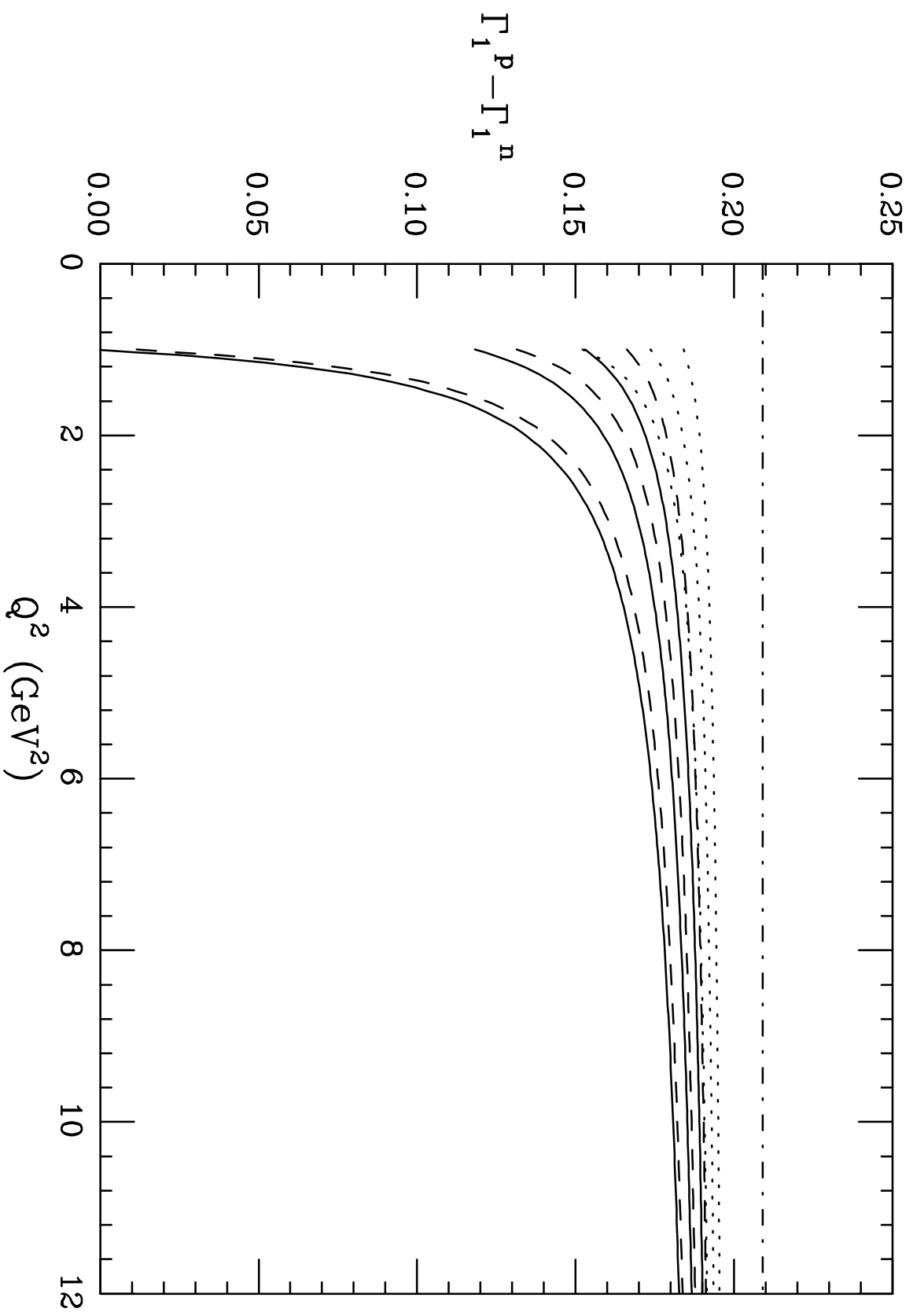


Fig. 5



This figure "fig1-6.png" is available in "png" format from:

<http://arxiv.org/ps/hep-ph/9409416v2>

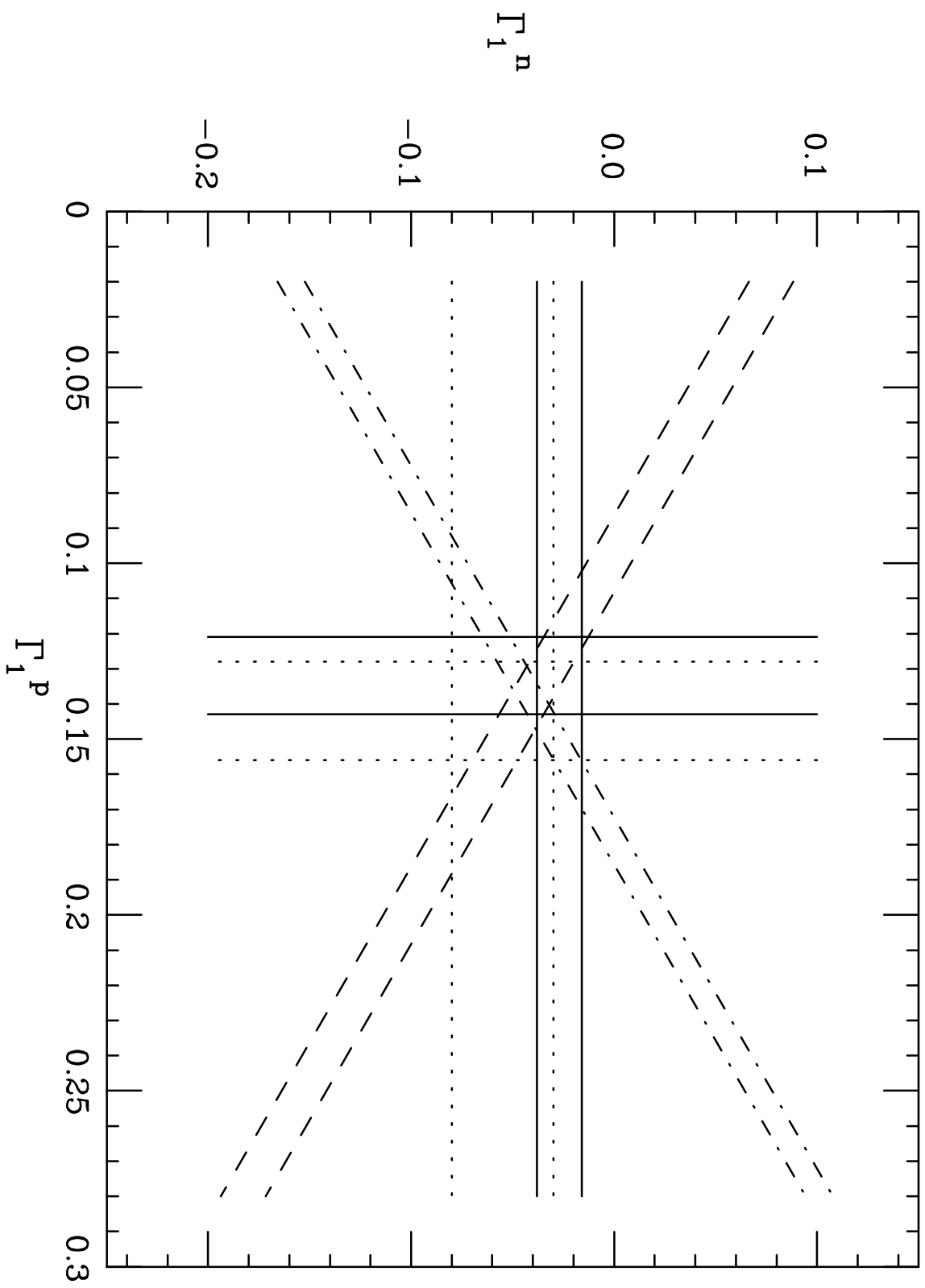


Fig. 6